

Neutron magnetic form factor in strongly correlated materials

Maria Elisabetta Pezzoli¹, Kristjan Haule¹, and Gabriel Kotliar¹

¹*Serin Physics Laboratory, Rutgers University,
Piscataway, NJ 08854, USA.*

(Dated: February 23, 2024)

We introduce a formalism to compute the neutron magnetic form factor $\mathbf{F}_M(\mathbf{q})$ within a first-principles Density Functional Theory (DFT) + Dynamical Mean Field Theory (DMFT). The approach treats spin and orbital interactions on the same footing and reduces to earlier methods in the fully localized or the fully itinerant limit. We test the method on various actinides of current interest NpCoGa₅, PuSb and PuCoGa₅, and we show that PuCoGa₅ is in mixed valent state, which naturally explains the measured magnetic form factor.

PACS numbers: 71.27.+a, 74.20.Mn, 75.25.-j

Compounds including elements from the actinide series provide a beautiful illustration of the challenges posed by correlated materials. The $5f$ electrons in these systems display simultaneously itinerant (i.e. band-like) and localized (atomic-like) properties. Describing the impact of this wave-particle duality on different physical observables, measured using different spectroscopic probes, is an outstanding theoretical challenge.

Neutron scattering[1] is a time-honored probe to investigate the dynamics of the magnetic degrees of freedom. It probes the dynamic susceptibility, describing the spatial and temporal distribution of magnetic fluctuations. In the itinerant limit, it can be modeled in terms of a particle hole continuum of quasiparticles, while in the localized limit it can be describe in terms of propagating spin waves. It is generally accepted that in many materials neither a fully itinerant nor a fully localized picture is adequate and some combination of both is required to model the dynamics of the spin fluctuations as in the duality model of Ref. 2.

The intensity in the magnetic Bragg peaks can be used to obtain a real picture of the magnetization inside the unit cell. This can be done even for materials that do not exhibit magnetic long range order, by applying an external magnetic field. Classical techniques can handle a fully itinerant or a fully localized picture [3]. However these approaches are not sufficient for many compounds of considerable scientific interest. It has been known for a while that intermediate valence rare-earth semiconductors show puzzling magnetic properties that can be explained only by a theory which explicitly considers the spatial extend of the magnetic excitations [4]. Similarly only magnetic orbitals of strong covalent nature can correctly account for the neutron intensity in the cuprates [5]. A theory able to describe the magnetic form factor for partly itinerant systems from first principles is needed.

Important recent experiments of Hiess *et. al.* determined the magnetic field induced form factor of PuCoGa₅, a material which superconducts at the remark-

ably high transition temperature $T_c \simeq 18.5$ K, a record in the heavy-fermion family [6]. The degree of itinerancy of the f electrons is the subject of active debate and has important consequences for the mechanism of superconductivity. Neither the localized nor the itinerant model of the neutron form factors fits the data well, providing strong motivation for our theoretical developments.

In this letter we develop a method to compute the form factor for magnetic neutron scattering within DFT+DMFT [7]. We test the method on several actinide materials. The PuCoGa₅ induced magnetic form factor is consistent with correlated mixed valent nature of the material, where both the $5f^5$ and $5f^6$ configuration are important. This is reminiscent of the mixed valent nature of elemental plutonium [8].

The magnetic form factor $\mathbf{F}_M(\mathbf{q})$ is defined by

$$\mathbf{F}_M(\mathbf{q}) = -\frac{1}{2\mu_B} \langle \mathbf{M}_T(\mathbf{q}) \rangle, \quad (1)$$

where $\mathbf{M}_T(\mathbf{q}) = \mathbf{M}_T^{\text{spin}}(\mathbf{q}) + \mathbf{M}_T^{\text{orb}}(\mathbf{q})$ is the Fourier transform of the transverse component of the magnetization density $\hat{q} \times (\mathbf{M}(\mathbf{r}) \times \hat{q})$, μ_B is the Bohr magneton and \mathbf{q} is the scattering wave vector at the Bragg peak. To avoid ambiguity in definition of magnetization [9], we express the form factor in terms of the Fourier transform of the current density $\mathbf{J}(\mathbf{q}) = \int d\mathbf{r} e^{-i\mathbf{q}\cdot\mathbf{r}} \mathbf{J}(\mathbf{r})$. The current and the transverse magnetization are related by $\mathbf{M}_T(\mathbf{q}) = \frac{i}{c} \mathbf{q} \times \mathbf{J}(\mathbf{q})/q^2$. The current has two contributions, the spin part $\mathbf{J}_{\text{spin}}(\mathbf{r})$ and the orbital part $\mathbf{J}_{\text{orb}}(\mathbf{r})$. Expressing the definition of $\mathbf{J}_{\text{orb}}(\mathbf{r})$ and $\mathbf{J}_{\text{spin}}(\mathbf{r})$ in terms of field operators $\Psi_s(\mathbf{r})$, we find for the form factor the following expression

$$\mathbf{F}_M(\mathbf{q}) = \frac{1}{q^2} \sum_{ss'} \int d\mathbf{r} e^{-i\mathbf{q}\cdot\mathbf{r}} \times \Psi_s^\dagger(\mathbf{r}) \mathbf{q} \times \left[\frac{1}{2} \vec{\sigma}_{ss'} \times \mathbf{q} + \delta_{ss'} \vec{\nabla} \right] \Psi_{s'}(\mathbf{r}), \quad (2)$$

where $\vec{\sigma}$ is the vector of the Pauli matrices and s, s' are the spin indexes. For a more detailed derivation see the

on-line supplementary material [10]. It is useful to notice that the limit $\lim_{q \rightarrow 0} \mathbf{F}_M(\mathbf{q})$ can be well defined, but it is subtle [11]. However the form factor $\mathbf{F}_M(\mathbf{q})$ is measured only at finite \mathbf{q} values and hence it is free from ambiguities.

$\mathbf{F}_M(\mathbf{q})$ is measured in polarized-neutron diffraction experiments directly through the *flipping ratio* technique. In this method an external magnetic field \mathbf{B} is applied to the sample, and the ratio $R = (d\sigma/d\Omega)_+ / (d\sigma/d\Omega)_-$ between the cross section for neutrons polarized parallel and anti-parallel to \mathbf{B} is measured. In a centrosymmetric crystal structure with collinear magnetic moments and $\mathbf{q} \perp \mathbf{B}$ the flipping ratio R satisfies $\left(\frac{\sqrt{R}-1}{\sqrt{R}+1}\right) = \gamma r_0 F_M(\mathbf{q})/b$ where b is the known nuclear scattering amplitude, $F_M(\mathbf{q})$ the component of the magnetic structure factor parallel to \mathbf{B} , $\gamma = 1.9132$ and $r_0 = \hbar e^2/mc^2$ is the classical electron radius. More general formulas which relate the form factor to the flipping ratio for other crystal structures and experimental setups are given in Ref. 12. For localized electrons the form factor is commonly fitted to the following radial dependence $F_M(q) = -\frac{\mu}{2\mu_B}(\langle j_0(q) \rangle + C_2 \langle j_2(q) \rangle)$, where $\langle j_k(q) \rangle$ stands for the spatial average over the atomic wave function of the magnetic atom (which is usually solved in the isolation). This should be understood in the so called *dipole approximation*. The exponent $e^{-i\vec{q}\cdot\vec{r}}$ is expanded around the center of the atom as $e^{-i\vec{q}\cdot\vec{r}} \approx j_0(qr) - i(\vec{q} \cdot \vec{r})(j_0(qr) + j_2(qr))$, where $j_k(qr)$ are spherical Bessel functions of order k . Within this approximation, the form factor is greatly simplified and in the common experimental set up ($\mathbf{q} \perp \mathbf{B}$, $\mathbf{B} = B\hat{\mathbf{z}}$), it reduces to

$$F_M(q) = \left\langle s_z j_0(qr) + \frac{1}{2} l_z \{j_0(qr) + j_2(qr)\} \right\rangle. \quad (3)$$

Here r is the distance from the magnetic atom, and $\langle \dots \rangle$ stands for the spatial and temporal average. The first and the second term in Eq. (3) come from the spin and the orbital contribution, respectively. The comparison of the above expansion with Eq. (3) shows that $\mu = -\mu_B \langle 2s_z + l_z \rangle$ and $\mu C_2 = -\mu_B \langle l_z \rangle$, hence $C_2 = \mu_L/(\mu_L + \mu_S)$. Clearly the ratio C_2 , which is given by the shape of the form factor, uniquely determines the size of the orbital and spin component within the dipole approximation. Even so, caution is necessary in interpreting experiments with Eq. (3), since a priori the magnitude of higher order terms beyond the dipole approximation is not known [13, 14].

To compute the form factor within DFT+DMFT, we apply a small magnetic field $\mathbf{B} = B\hat{\mathbf{z}}$ to induce a finite magnetic moment. We solve the DMFT problem in the presence of magnetic field, and evaluate the correlation function Eq. (2). When expressed in the Kohn-Sham

basis, Eq. (2) takes the form

$$\mathbf{F}_M(\mathbf{q}) = \frac{1}{q^2} \sum_{\mathbf{k}, ij, ss'} n_{\mathbf{k}, ij}^{\text{DMFT}} \times \int_{\text{unit cell}} d\mathbf{r} e^{-i\mathbf{q}\cdot\mathbf{r}} \psi_{\mathbf{k}i}^*(\mathbf{r}, s) \mathbf{q} \times \left[\frac{1}{2} \vec{\sigma}_{ss'} \times \mathbf{q} + \delta_{ss'} \vec{\nabla} \right] \psi_{\mathbf{k}j}(\mathbf{r}, s'), \quad (4)$$

where $\psi_{\mathbf{k}i}(\mathbf{r}, s)$ are the Kohn-Sham orbitals, i runs over the Kohn-Sham bands, and \mathbf{k} over the first Brillouin zone. The “DMFT density matrix” $n_{\mathbf{k}, ij}^{\text{DMFT}}$ is expressed in terms of the DMFT Green function $G_{ij}(\mathbf{k}, \omega)$ in the solid $n_{ij\mathbf{k}}^{\text{DMFT}} = \frac{1}{2\pi i} \int d\omega (G_{ij}^*(\mathbf{k}, \omega) - G_{ji}(\mathbf{k}, \omega)) f(\omega)$, where $f(\omega)$ is the Fermi function. The form factor is thus expressed in terms of the one particle correlation function, which is easily accessible within DMFT. Moreover, the spatial integral is local and runs over one unit cell, which makes local DMFT approximation particularly suitable for this problem. We implemented Eq. (4) within the recent realization of DFT+DMFT [15] based on Linear Augmented Plane Wave (LAPW) basis set as implemented in the full potential electronic structure code Wien2k [16]. The explicit formulas for the form factor evaluation within this basis set, as well as detail derivation of Eq. (4) are given in the on line material [10]. To solve the impurity problem in the presence of magnetic field, we used the Non-Crossing Approximation [15]. Our calculations show small anisotropic corrections to dipole approximation for the materials studied here, suggesting that the dipole approximation is a good approximation for these compounds. For comparison, we also compute the form factor within Local Spin Density Approximation (LSDA) as first discussed in Ref. 17. In practice we evaluate the mean value of Eq. (3) inside the atomic sphere following the lines of Ref. 18. We perform the LSDA calculation in the presence of external magnetic field, as implemented in Wien2K [19].

In Fig. 1(A) we compare theoretical DFT+DMFT and LSDA form factors with experiments on NpCoGa₅ in the paramagnetic state [6]. Our DFT+DMFT form factor is in excellent agreement with experiment, while the LSDA dramatically fails in this material. The LSDA form factor shows a minimum at finite wave vector \mathbf{q} . Such a large minimum can be explained by $C_2 \sim -9.5$; this occurs since μ_L and μ_s almost cancel, but $|\mu_L| < |\mu_s|$. An underestimation of the orbital moment is typical of LSDA. Within DFT+DMFT the atomic degrees of freedom are treated exactly by the exact diagonalization of the atomic 5f-shell in the presence of magnetic field. This ensures that Hund’s rule coupling is properly treated, leading to anti-parallel μ_L and μ_S , but $|\mu_L| > |\mu_S|$, hence $C_2 > 0$. For NpCoGa₅ we determine the value of the coefficient $C_2 = 2.16$. This value is consistent with localized 5f-electrons in the configuration 5f⁴, in agreement with Mössbauer spectroscopy [20] and neutron diffraction experiments [6, 21]. At the same time NMR [22] and inelas-

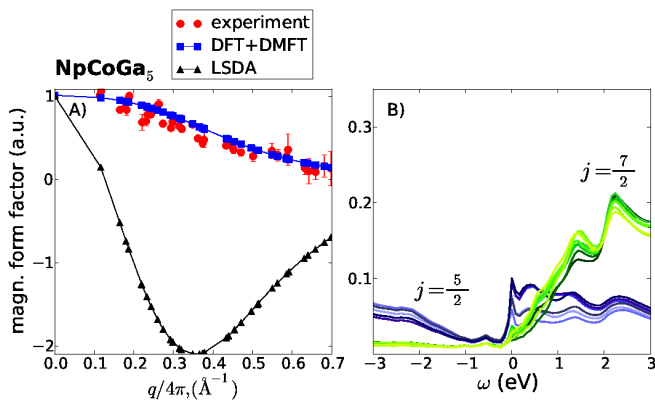


FIG. 1: (Color on line) A) panel: magnetic form factor for NpCoGa_5 . Red dots are experimental data reproduced from 6. The blue curve with squares is the DFT+DMFT calculation, and the black curve with triangles is the LSDA calculation. The DFT+DMFT form factor agrees with experiment with value of the Pearson correlation coefficient $R_{\text{PMCC}} = 0.95$. B) panel: spectral function $A_{jm_j}(\omega)$ for Np f-electrons. Blue curves correspond to the $j = 5/2$ multiplet and green curves to the $j = 7/2$ multiplet. The experimental and theoretical DMFT temperature is $T = 52$ K.

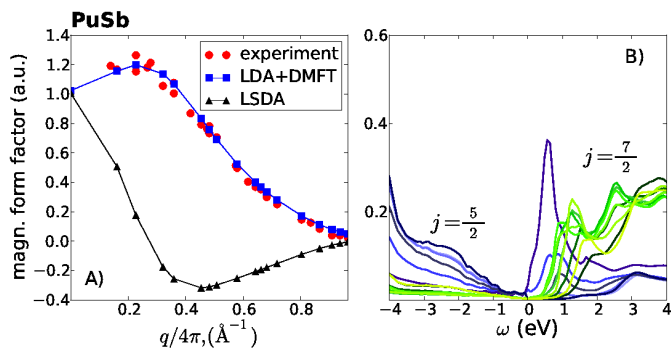


FIG. 2: (Color on line) A) panel: magnetic form factor for PuSb at $T = 20$ K. Red dots are experimental data [24], the blue curve with square is the DFT+DMFT calculation and the black curve with triangles the LSDA calculation. The DFT+DMFT curve agrees with experiment with a Pearson Correlation coefficient $R_{\text{PMCC}} = 0.95$. B) panel: Spectral function for PuSb . The color legend is the same as in Fig. 1.

tic neutron scattering [23] suggest that NpCoGa_5 shows also itinerant aspects of the $5f$ -electrons. A signature of this moderate delocalization is also apparent in our calculated spectral function at $T = 52$ K displayed in Fig. 1(B). A small quasiparticle peak is formed at the Fermi level, a signature of electron itinerancy at low energy. Next we compute the form factor for PuSb in the ferromagnetic state. PuSb is a metal [25], which orders antiferromagnetically below $T_N = 85$ K and becomes a ferromagnet at $T = 67$ K [26]. Theoretically it has been showed that in PuSb valence fluctuations are sup-

pressed with the consequent absence of a quasiparticle multiplet structure in the spectral function [27]. This result is consistent with neutron diffraction data: the form factor curve has a characteristic maximum at finite q , feature typical of a pure f^5 configuration state for the Pu atom [24]. The LSDA calculation underestimates the orbital moment and finds a negative C_2 coefficient. Our DFT+DMFT calculation reproduces the f -electrons occupation value $\langle n_f \rangle \sim 5.0$ of the previous experimental and theoretical works [24, 27] and indeed it is in good agreement with the measured data, see (see Fig. 2A). In particular we find that there is a large cancellation between orbital and spin moment with $\mu_S/\mu_L = -0.74$ and $C_2 = 3.92$. We now turn to PuCoGa_5 . Photo

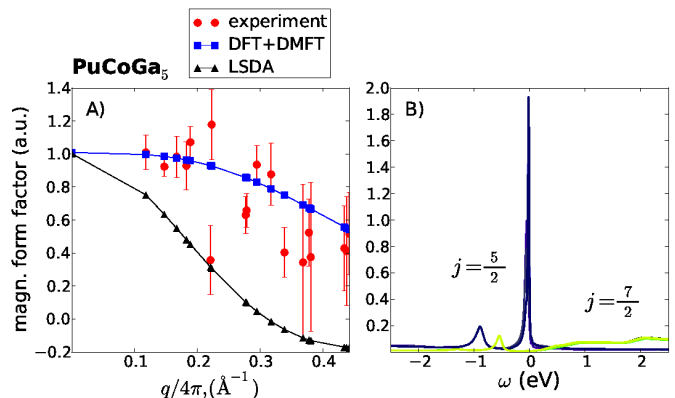


FIG. 3: (Color on line) A) panel : magnetic form factor for PuCoGa_5 . The blue curve with squares corresponds to the full DFT+DMFT calculation, the black curve with triangles to the LSDA calculation. Red dots are experimental data [6] The DFT+DMFT curve agrees with experiment with a Pearson correlation coefficient $R_{\text{PMCC}} = 0.70$. B) panel: spectral function $A_{jm_j}(\omega)$ for Pu f-electrons. The color legend is the same as in Fig. 1

emission spectra show the formation of a quasiparticle peak at the Fermi level, however there is a large discrepancy in the peak height between different measurements [28, 29]. First magnetic susceptibility measurements suggested that $5f$ -electrons behave as unquenched local moments until they enter in the superconducting state [30]. In turn neutron scattering shows a temperature independent magnetic susceptibility, implying the absence of magnetic moments such as in δ - Pu [6, 31]. Electronic structure calculations qualitatively support the picture of delocalized $5f$ -states, however they predict a Pu ion close to magnetic order and a form factor shape not observed in experiments [32, 33]. Since our understanding of superconductivity in PuCoGa_5 depends on the itinerant or localized nature of correlated electrons [34], further theoretical and experimental investigations are compelling. Within our DFT+DMFT calculation we find that a quasiparticle peak appears at the Fermi level, see Fig. 3(B). These results are consistent with a specific

heat coefficient $\gamma \sim 70 \text{ mJ}/(K^2 \text{ mol})$, which compares well with experiments [30], and go beyond the pioneer DFT+DMFT calculations, solved within the T-matrix and fluctuating exchange technique [35]. Together with a quasiparticle peak, a mixed valent state forms, where the $5f$ -electrons have a finite probability to be both in the configuration state f^5 and f^6 . Our theoretical prediction for the $5f^6$ occupation probability is $P_{f^6} = 0.26$, corresponding to $\langle n_f \rangle \sim 5.26$ and a coefficient $C_2 = 2.35$. We plot the corresponding form factor curve in Fig. 3(A) together with the form factor obtained from the LSDA calculation. As for the previous materials, LSDA underestimates the orbital moment and it obtains a negative C_2 coefficient that is inconsistent with experimental data. The DFT+DMFT form factor with $C_2 = 2.35$ well describes the neutrons data and it accounts also for the magnetic susceptibility (see the supplementary material [10]). The value of $C_2 = 2.35$ is naturally explained by the mixed valence picture obtained theoretically for PuCoGa_5 . For a free Pu^{3+} ion solved in the intermediate coupling $C_2 = 3.83$, hence $\mu_L/\mu_S = -1.83$ [3]; As a mixture of the configuration f^6 is included in the many body ground state, the ratio μ_L/μ_S becomes more negative and therefore C_2 decreases. As pointed out in Ref. 6 the $F_M(q)$ shape is very different from the one expected for a pure $5f^5$ configuration of an isolated Pu ion, as for example is found in PuSb , see Fig. 2(a). At the same time it is very different from the LSDA prediction. Hence, the magnetic properties of PuCoGa_5 are not captured either by a free moment picture or by an itinerant picture.

In conclusion in this letter we presented a new approach to compute the neutron magnetic form factor. The LSDA treatment fails to reproduce the correct form factor since the exchange energy is orbital-independent and therefore Hund's rules are not respected. On the contrary DFT+DMFT includes the atomic physics needed to describe strongly correlated systems. Application of DFT+DMFT to PuCoGa_5 suggest an explanation of the results of Ref. 6 in terms of a mixed valence picture where the ground state of Pu fluctuates between two distinct configurations: f^5 and f^6 . We indeed checked that this picture accounts for the values of the specific heat and susceptibility as well as for the shape of photoemission spectra. We find a close similarity between the DFT+DMFT valence histogram of PuCoGa_5 and δ -Pu, suggesting a close analogy of the local physics in these two materials; the magnetic form factor of PuCoGa_5 would then be very similar to that of δ -Pu, for which experiments are notoriously difficult. Finally, mixed valence is an attractive mechanism for pairing in heavy fermions [36], which could account for the high temperature superconductivity in PuCoGa_5 . *Acknowledgment:* We would like to thank G. Lander and A. Hiess for numerous discussions of this problem, and for providing us the raw data of his scattering experiments which are plotted in this work. We thank M. Dzero for an early col-

laboration in the initial stage of this work. The work of M. Pezzoli and G. Kotliar was supported by BES DOE-grant BES-DOE Grant DE-FG02-99ER45761. K. Haule acknowledges the support of ACS Petroleum Research Fund 48802 and Alfred P. Sloan foundation.

-
- [1] S. Lovesey and D. Rimmer, Rep. Prog. Phys **32**, 333 (1969).
 - [2] K. Miyake and Y. Kuramoto, Physica B: Condensed Matter **171**, 20 (1991).
 - [3] G. Lander, *Handbook of the Physics and Chemistry of Rare Earths*, vol. 17 (Elsevier, 1993).
 - [4] K. Kikoin and A. Mishchenko, J. Phys. Cond. Matt. **7**, 307 (1995).
 - [5] A. C. Walters et al., Nat. Phys. **5**, 867 (2009).
 - [6] A. Hiess et al., Phys. Rev. Lett. **100**, 076403 (2008).
 - [7] G. Kotliar et al., Rev. Mod. Phys. **78**, 865 (2006).
 - [8] J. Shim, K. Haule, and G. Kotliar, Nature **446**, 513 (2007).
 - [9] L. L. Hirst, Rev. Mod. Phys. **69**, 607 (1997).
 - [10] See EPAPS Document No. XXX for a detailed derivation of the form factor formulas in the LAPW basis set and of the dipole approximation.
 - [11] T. Thonhauser, D. Ceresoli, D. Vanderbilt, and R. Resta, Phys. Rev. Lett. **95**, 137205 (2005).
 - [12] E. Balcar and S. Lovesey, eds., *Theory of Magnetic Neutron and Photon Scattering* (Oxford University Press, New York, 1989).
 - [13] M. Rotter and A. T. Boothroyd, Phys. Rev. B **79**, 140405 (2009).
 - [14] K. Ayuel and P. F. de Châtel, Phys. Rev. B **61**, 15213 (2000).
 - [15] K. Haule, C.-H. Yee, and K. Kim, Phys. Rev. B **81**, 195107 (2010).
 - [16] P. Blaha, K. Schwarz, G. Madsen, K. Kvasnicka, and J. Luitz, *Wien2k*, Karlheinz Schwarz, Technische Universität Wien, Austria (2001).
 - [17] A. J. Freeman, Phys. Scr. **15**, 80 (1977).
 - [18] M. S. S. Brooks and P. J. Kelly, Phys. Rev. Lett. **51**, 1708 (1983).
 - [19] We used *orb* subroutine in Wien2K, as implemented by Pavel Novak.
 - [20] N. Metoki et al., Phys. Rev. B **72**, 014460 (2005).
 - [21] E. Colineau et al., Phys. Rev. B **69**, 184411 (2004).
 - [22] H. Sakai et al., Phys. Rev. B **76**, 024410 (2007).
 - [23] N. Magnani et al., Phys. Rev. B **76**, 100404 (2007).
 - [24] G. H. Lander et al., Phys. Rev. Lett. **53**, 2262 (1984).
 - [25] A. Blaise et al., Physica B+C **130**, 99 (1985).
 - [26] P. Burlet et al., Phys. Rev. B **30**, 6660 (1984).
 - [27] C.-H. Yee, G. Kotliar, and K. Haule, Phys. Rev. B **81**, 035105 (2010).
 - [28] R. Eloirdi et al., Journal of Nucl. Mater. **385**, 8 (2009).
 - [29] J. J. Joyce et al., Phys. Rev. Lett. **91**, 176401 (2003).
 - [30] J. Sarrao et al., Nature **420**, 297 (2002).
 - [31] J. C. Lashley, A. Lawson, R. J. McQueeney, and G. H. Lander, Phys. Rev. B **72**, 054416 (2005).
 - [32] I. Opahle and P. M. Oppeneer, Phys. Rev. Lett. **90**, 157001 (2003).
 - [33] A. B. Shick, V. Janis, and P. M. Oppeneer, Phys. Rev. Lett. **94**, 016401 (2005).

- [34] R. Flint, M. Dzero, and P. Coleman, Nat. Phys. **4**, 643 (2008). [36] K. Miyake, O. Narikiyo, and Y. Onishi, Physica B **259**, 676 (1999).
 [35] L. V. Pourovskii, M. I. Katsnelson, and A. I. Lichtenstein, Phys. Rev. B **73**, 060506 (2006).

Supplementary Material

FORM FACTOR IN SECOND QUANTIZATION

The neutron magnetic form factor can be evaluated in terms of current $\vec{J}(\vec{r})$ by the following formula

$$\vec{F}_M(\vec{q}) = \frac{im_e}{e\hbar} \frac{1}{q^2} \vec{q} \times \langle \vec{J}(\vec{q}) \rangle, \quad (\text{S1})$$

where m_e , e are respectively the electron mass and the electron charge ($e < 0$), \vec{q} is the scattering wave vector and

$$\vec{J}(\vec{q}) = \int d\vec{r} e^{-i\vec{q}\cdot\vec{r}} (\vec{J}_{\text{orb}}(\vec{r}) + \vec{J}_{\text{spin}}(\vec{r})). \quad (\text{S2})$$

The orbital and spin currents in terms of the field operators $\Psi_s(\vec{r})$ are given by

$$\vec{J}_{\text{orb}}(\vec{r}) = \frac{e\hbar}{2im_e} \sum_s \left[\Psi_s^\dagger(\vec{r}) (\vec{\nabla} \Psi_s(\vec{r})) - (\vec{\nabla} \Psi_s^\dagger(\vec{r})) \Psi_s(\vec{r}) \right] \quad (\text{S3})$$

$$\vec{J}_{\text{spin}}(\vec{r}) = \frac{e\hbar}{2m_e} \sum_{ss'} \left[\Psi_s^\dagger(\vec{r}) (\vec{\nabla} \Psi_{s'}(\vec{r})) + (\vec{\nabla} \Psi_s^\dagger(\vec{r})) \Psi_{s'}(\vec{r}) \right] \times \vec{\sigma}_{ss'}. \quad (\text{S4})$$

Note that the Fourier transform of the spin current $\vec{J}_{\text{spin}}(\vec{q})$ greatly simplifies: in fact integration by parts leads to cancellation of the derivatives of the field operator and we obtain $\vec{J}_{\text{spin}}(\vec{q}) = -e\hbar i/(2m_e) \sum_{ss'} \vec{\sigma}_{ss'} \rho_{ss'}(\vec{q}) \times \vec{q}$. Inserting the expression for the currents into Eq. (S1), we get

$$\vec{F}_M(\vec{q}) = \frac{1}{q^2} \sum_{ss'} \int d\vec{r} e^{-i\vec{q}\cdot\vec{r}} \Psi_s^\dagger(\vec{r}) \vec{q} \times \left[\frac{1}{2} \vec{\sigma}_{ss'} \times \vec{q} + \delta_{ss'} \vec{\nabla} \right] \Psi_{s'}(\vec{r}) \quad (\text{S5})$$

Now we express the field operator in terms of a complete set of one particle wave functions, such as Kohn-Sham orbitals

$$\Psi_s(\vec{r}) = \sum_{i \in \text{band}, \vec{k} \in \text{BZ}} \psi_{ki}(\vec{r}, s) \hat{c}_{\vec{k}i}, \quad (\text{S6})$$

to get

$$\vec{F}_M(\vec{q}) = \frac{1}{q^2} \sum_{\vec{k}, ij, ss'} n_{\vec{k}, ij}^{DMFT} \int_{\text{cell}} d\vec{r} e^{-i\vec{q}\cdot\vec{r}} \psi_{ki}^*(\vec{r}, s) \vec{q} \times \left[\frac{1}{2} \vec{\sigma}_{ss'} \times \vec{q} + \delta_{ss'} \vec{\nabla} \right] \psi_{kj}(\vec{r}, s') \quad (\text{S7})$$

Here $n_{\vec{k}, ij}^{DMFT}$ is the DMFT density matrix expressed in the Kohn-Sham base, \vec{k} runs over the first Brillouin zone only, and i, j run over Kohn-Sham bands. Because \vec{q} is reciprocal vector, the integration over space is performed only over one unit cell (denoted by *cell*). When the spin-orbit coupling is large, bands do not have the spin index, because there is mixing between both spins species, hence we need to double the number of bands.

In the LAPW basis, there are two contributions to the above equation: within muffin-tin and in the interstitial region.

Within Muffin-Tin

Inside the Muffin-Tin the KS orbitals are expressed in terms of coefficients $A_{i, \vec{K}s}^{\vec{k}}$ and LAPW basis functions $\chi_{\vec{k}+\vec{K}}(\vec{r}, s)$ as

$$\psi_{ki}(\vec{r}, s) = \sum_{\vec{K}} A_{i, \vec{K}s}^{\vec{k}} \chi_{\vec{k}+\vec{K}}(\vec{r}, s) = \sum_{\vec{K}s} A_{i, \vec{K}s}^{\vec{k}} a_{\vec{L}\vec{K}}^{\vec{k}kt} u_l^{\kappa t}(r_t) Y_L(\hat{r}_t) \chi_s, \quad (\text{S8})$$

where \vec{K} are reciprocal lattice vectors, t marks the atom type, $u_l^{0t}(r)$, $u_l^{1t}(r)$, $u_l^{2t}(r)$ are the radial solutions of the Dirac equation, its energy derivative, and optional local orbitals; $Y_L(\hat{r}_t)$ are spherical harmonics with L labeling the angular quantum numbers l, m .

For shorter notation, we define a new type of density matrix in the muffin-tin subspace

$$n_{\vec{k},t,Ls\kappa,L's'\kappa'}^{DMFT} = \sum_{ij} \left(\sum_{\vec{K}} A_{i,\vec{K}s}^{\vec{k}*} a_{L\vec{K}}^{\vec{k}\kappa t*} \right) n_{\vec{k},ij}^{DMFT} \left(\sum_{\vec{K}'} A_{j,\vec{K}'s'}^{\vec{k}} a_{L'\vec{K}'}^{\vec{k}\kappa't} \right) \quad (S9)$$

and we express the form factor inside the muffin-tin in terms of this density matrix

$$\vec{F}_M(\vec{q}) = \frac{1}{q^2} \sum_{\vec{k},t,Ls\kappa,L's'\kappa'} n_{\vec{k},t,Ls\kappa,L's'\kappa'}^{DMFT} \langle u_l^\kappa Y_L \chi_s | e^{-i\vec{q}\vec{r}} \left[\frac{1}{2} \vec{q} \times (\vec{\sigma}_{ss'} \times \vec{q}) + \delta_{ss'} \vec{q} \times \vec{\nabla} \right] | u_{l'}^{\kappa'} Y_{L'} \chi_{s'} \rangle_t \quad (S10)$$

Here integration runs over muffin-tin sphere t .

From the above expression it is not obvious that the $q \rightarrow 0$ is well behaved. However, we can add any constant to exponent $e^{i\vec{q}\cdot\vec{r}}$ in the orbital part of the expression, because it vanishes due to symmetry. It is therefore possible to write an alternative expression

$$\vec{F}_M^{MT}(\vec{q}) = \frac{1}{q^2} \sum_{\vec{k},t,Ls\kappa,L's'\kappa'} n_{\vec{k},t,Ls\kappa,L's'\kappa'}^{DMFT} \langle u_l^\kappa Y_L \chi_s | \left[\frac{1}{2} e^{-i\vec{q}\vec{r}} \vec{q} \times (\vec{\sigma}_{ss'} \times \vec{q}) + \delta_{ss'} (e^{-i\vec{q}\vec{r}} - 1) \vec{q} \times \vec{\nabla} \right] | u_{l'}^{\kappa'} Y_{L'} \chi_{s'} \rangle_t \quad (S11)$$

which clearly is well behaved in the $\vec{q} = 0$ limit.

Interstitial Region

In the interstitial region the KS solution is

$$\psi_{\vec{k}i}(\vec{r}, s) = \sum_{\vec{K}} A_{i,\vec{K}s}^{\vec{k}} \frac{1}{\sqrt{V_{cell}}} C_{\vec{K}} e^{i(\vec{k}+\vec{K})\vec{r}} \chi_s \quad (S12)$$

We again define a corresponding density matrix

$$n_{\vec{k},\vec{K}s,\vec{K}'s'}^{DMFT} = \sum_{ij} A_{i,\vec{K}s}^{\vec{k}*} C_{\vec{K}}^* n_{\vec{k},ij}^{DMFT} A_{j,\vec{K}'s'}^{\vec{k}} C_{\vec{K}'}, \quad (S13)$$

and express the form factor by

$$\begin{aligned} \vec{F}_M^I(\vec{q}) &= \frac{1}{q^2} \sum_{\vec{k},\vec{K}s,\vec{K}'s'} n_{\vec{k},\vec{K}s,\vec{K}'s'}^{DMFT} \\ &\times \left[\frac{1}{2} \vec{q} \times (\vec{\sigma}_{ss'} \times \vec{q}) + i \delta_{ss'} \vec{q} \times \left(\vec{k} + \frac{1}{2} \vec{K} + \frac{1}{2} \vec{K}' \right) \right] \left[\delta_{\vec{K}'-\vec{K}-\vec{q}} - \sum_t \frac{4\pi R_t^2}{V_{cell}} \frac{j_1(|\vec{K}'-\vec{K}-\vec{q}| R_t)}{|\vec{K}'-\vec{K}-\vec{q}|} \right] \end{aligned} \quad (S14)$$

The last term comes from the difference of the integral over the entire unit cell and inside all muffin-tin spheres.

DIPOLE APPROXIMATION

In the dipole approximation, we approximate the Fourier exponent with

$$e^{-i\vec{q}\vec{r}} \approx j_0(qr) - i(\vec{q} \cdot \vec{r})(j_0(qr) + j_2(qr)) \quad (S15)$$

and obtain

$$\vec{F}_M(\vec{q}) = \frac{1}{q^2} \sum_{\vec{k},ij,ss'} n_{\vec{k},ij}^{DMFT} \int_{cell} d\vec{r} [j_0(qr) - i(\vec{q} \cdot \vec{r})(j_0(qr) + j_2(qr))] \psi_{\vec{k}i}^*(\vec{r}, s) \vec{q} \times \left[\frac{1}{2} \vec{\sigma}_{ss'} \times \vec{q} + \delta_{ss'} \vec{\nabla} \right] \psi_{\vec{k}j}(\vec{r}, s') \quad (S16)$$

Due to parity selection rules, only the following two terms are nonzero

$$\begin{aligned} \vec{F}_M(\vec{q}) &= \frac{1}{q^2} \sum_{\vec{k}, ij, ss'} n_{\vec{k}, ij}^{DMFT} \\ &\times \int_{cell} d\vec{r} \psi_{ki}^*(\vec{r}, s) \left[j_0(qr) \frac{1}{2} \vec{q} \times (\vec{\sigma}_{ss'} \times \vec{q}) - i\delta_{ss'} [j_o(qr) + j_2(qr)] (\vec{q} \cdot \vec{r}) (\vec{q} \times \vec{\nabla}) \right] \psi_{kj}(\vec{r}, s'). \end{aligned} \quad (S17)$$

Inside the expression Eq. (S17) for form factor, we can use

$$-i(\vec{q} \cdot \vec{r}) (\vec{q} \times \vec{\nabla}) = \frac{1}{2} \frac{m_e}{\hbar} \frac{d}{dt} [(\vec{q} \cdot \vec{r}) (\vec{q} \times \vec{r})] - \frac{1}{2} i(\vec{q} \cdot \vec{r}) (\vec{q} \times \vec{\nabla}) + \frac{1}{2} i(\vec{q} \cdot \vec{\nabla}) (\vec{q} \times \vec{r}).$$

The following term vanishes

$$\sum_{\vec{k}, ij} n_{\vec{k}, ij}^{DMFT} \langle \psi_{ik} | \frac{1}{2} \frac{m_e}{\hbar} \frac{d}{dt} [(\vec{q} \cdot \vec{r}) (\vec{q} \times \vec{r})] | \psi_{jk} \rangle = \left\langle \frac{1}{2} \frac{m_e}{\hbar} \frac{d}{dt} [(\vec{q} \cdot \vec{r}) (\vec{q} \times \vec{r})] \right\rangle = 0. \quad (S18)$$

Hence we can use

$$- \frac{1}{2} i(\vec{q} \cdot \vec{r}) (\vec{q} \times \vec{\nabla}) + \frac{1}{2} i(\vec{q} \cdot \vec{\nabla}) (\vec{q} \times \vec{r}) = \frac{i}{2} \vec{q} \times [\vec{q} \times (\vec{r} \times \vec{\nabla})] \quad (S19)$$

and $\vec{r} \times \vec{\nabla} = \frac{i}{\hbar} \vec{l}$ to write

$$i(\vec{q} \cdot \vec{r}) (\vec{q} \times \vec{\nabla}) = \frac{1}{2\hbar} \vec{q} \times (\vec{l} \times \vec{q}); \quad (S20)$$

Finally we find the expression for the form factor in the dipole approximation

$$\begin{aligned} \vec{F}_M(\vec{q}) &= \frac{1}{q^2} \sum_{\vec{k}, ij, ss'} n_{\vec{k}, ij}^{DMFT} \\ &\times \int_{cell} d\vec{r} \psi_{ki}^*(\vec{r}, s) \left[\frac{1}{2} \vec{q} \times (\vec{\sigma}_{ss'} \times \vec{q}) j_0(qr) + \delta_{ss'} \frac{1}{2\hbar} [(\vec{q} \times \vec{l}) \times \vec{q}] [j_o(qr) + j_2(qr)] \right] \psi_{kj}(\vec{r}, s'). \end{aligned} \quad (S21)$$

Inside the muffin-tin the Kohn Sham orbitals are expressed in terms of a basis in which \vec{l} and \vec{s} are diagonal. Therefore the form factor in the dipole approximation, inside the muffin-tin, reads

$$\vec{F}_M(\vec{q}) = \sum_{\vec{k}, t, s, L, \kappa, \kappa'} n_{\vec{k}, t, L, \kappa, L, \kappa'}^{DMFT} \frac{\vec{q} \times (\vec{e}_z \times \vec{q})}{q^2} \left[s_z \langle u_l^\kappa | j_0(qr) | u_l^{\kappa'} \rangle + \frac{1}{2} l_z \langle u_l^\kappa | j_o(qr) + j_2(qr) | u_l^{\kappa'} \rangle \right]. \quad (S22)$$

where we took the magnetic field in z direction.

NUMERICAL EVALUATION

For numerical evaluation we split the form factor expression into the dipole part and the correction to the dipole approximation ΔF_M . The correction is

$$\Delta \vec{F}_M(\vec{q}) = \frac{1}{q^2} \sum_{\vec{k}, ij, ss'} n_{\vec{k}, ij}^{DMFT} \langle \psi_{ki, s} | [e^{-i\vec{q}\vec{r}} - j_0(qr)] \frac{1}{2} \vec{q} \times (\vec{\sigma}_{ss'} \times \vec{q}) + \delta_{ss'} [e^{-i\vec{q}\vec{r}} + i(\vec{q} \cdot \vec{r}) (j_o(qr) + j_2(qr))] (\vec{q} \times \vec{\nabla}) | \psi_{kj, s'} \rangle.$$

Inside the muffin-tin sphere, this expression takes the form

$$\begin{aligned} \Delta \vec{F}_M(\vec{q}) &= \frac{1}{q^2} \sum_{\vec{k}, t, s, L, \kappa, L', \kappa'} n_{\vec{k}, L, \kappa, t, L', \kappa'}^{DMFT} \left\{ \vec{q} \times (\vec{e}_z \times \vec{q}) \frac{1}{2} \sigma_{ss}^z \langle u_l Y_L | [e^{-i\vec{q}\vec{r}} - j_0(qr)] | u_{l'} Y_{L'} \rangle \right. \\ &\quad \left. + \langle u_l Y_L | [e^{-i\vec{q}\vec{r}} - 1 + i(\vec{q} \cdot \vec{r}) (j_o(qr) + j_2(qr))] (\vec{q} \times \vec{\nabla}) | u_{l'} Y_{L'} \rangle \right\}. \end{aligned} \quad (S23)$$

We compute in advance the following quantities

$$a_{LL'}(r) = \langle Y_L | e^{-i\vec{q}\cdot\vec{r}} - 1 | Y_{L'} \rangle \quad (\text{S24})$$

$$b_{LL'}(r) = \langle Y_L | -i\vec{q}\cdot\vec{r} | Y_{L'} \rangle \quad (\text{S25})$$

$$\vec{c}_{LL'}(r) = \langle Y_L | \vec{q} \times \vec{\nabla} | Y_{L'} \rangle \quad (\text{S26})$$

$$\vec{d}_{LL'}(r) = \langle Y_L | \vec{q} \times \vec{e}_r | Y_{L'} \rangle \quad (\text{S27})$$

and obtain the following one dimensional integral over the radial distance in the muffin-tin sphere

$$\begin{aligned} \Delta \vec{F}_M(\vec{q}) = & \frac{1}{q^2} \sum_{\vec{k}, t, s, L\kappa, L'\kappa'} n_{\vec{k}, Ls\kappa t, L's\kappa' t}^{DMFT} \left\{ \vec{q} \times (\vec{e}_z \times \vec{q}) \frac{1}{2} \sigma_{ss}^z \int dr r^2 u_l^\kappa(r) u_{l'}^{\kappa'}(r) [a_{LL'}(r) + \delta_{LL'} (1 - j_0(qr))] \right. \\ & + \int dr r^2 u_l^\kappa(r) \frac{du_{l'}^{\kappa'}(r)}{dr} \sum_{L''} \{ a_{LL''}(r) - b_{LL''}(r) [j_0(qr) + j_2(qr)] \} \vec{d}_{L''L'}(r) \\ & \left. + \int dr r^2 u_l^\kappa(r) u_{l'}^{\kappa'}(r) \sum_{L''} \{ a_{LL''}(r) - b_{LL''}(r) [j_0(qr) + j_2(qr)] \} \vec{c}_{L''L'}(r) \right\}. \end{aligned} \quad (\text{S28})$$

To check numerical accuracy, one could check the accuracy of the following sum

$$\begin{aligned} \sum_{L''} b_{LL''} \vec{c}_{L''L'} &= \langle Y_L | -i(\vec{q}\cdot\vec{r})(\vec{q} \times \vec{\nabla}) | Y_{L'} \rangle = \\ &= -i\langle Y_L | (\vec{q} \times \vec{r})(\vec{q}\cdot\vec{\nabla}) - i\vec{q} \times (\vec{q} \times \vec{l}) | Y_{L'} \rangle = \\ &= -i\langle Y_L | (\vec{q} \times \vec{r})(\vec{q}\cdot\vec{\nabla}) | Y_{L'} \rangle - \vec{q} \times (\vec{q} \times \vec{e}_z) l_z \delta_{LL'}; \end{aligned}$$

since for $L = L'$ the first term is zero, we have

$$\sum_{L''} b_{LL''} \vec{c}_{L''L} = -\vec{q} \times (\vec{q} \times \vec{e}_z) l_z \quad (\text{S29})$$

To derive the above equation, it is useful to know the following property of the spherical harmonics

$$\frac{d}{d\theta} Y_{l,m}(\theta, \phi) = \frac{1}{2} \sqrt{(l-m)(l+m+1)} e^{-i\phi} Y_{l,m+1}(\theta, \phi) - \frac{1}{2} \sqrt{(l+m)(l-m+1)} e^{i\phi} Y_{l,m-1}(\theta, \phi) \quad (\text{S30})$$

which follows from

$$\sqrt{1-x^2} \frac{d}{dx} P_{l,m}(x) = -\frac{1}{2} P_{l,m+1}(x) + \frac{1}{2} (l+m)(l-m+1) P_{l,m-1}(x). \quad (\text{S31})$$

MAGNETIC SUSCEPTIBILITY FOR PuCoGa₅

From the calculation of the magnetic form factor $F_M(q)$ we can extract the magnetic susceptibility as $\chi = \mu/B$, where $\mu = -2\mu_B F_M(0)$ is the magnetic moment of the Pu atom and B is the applied magnetic field. The results are summarized in table I.

TABLE I: Magnetic susceptibility for PuCoGa₅ obtained with the NCA impurity solver.

T (Kelvin)	χ (μ_B /Tesla)
12.5	12×10^{-4}
25	13×10^{-4}
50	15×10^{-4}

The computed magnetic susceptibility compares well with the values obtained by the neutron experiment [A. Hiess *et al.*, Phys. Rev. Lett. **100**, 076403 (2008)]. DFT+DMFT obtains a larger susceptibility than the measured one, which is comprehensible since it is well known that the Non Crossing Approximation (NCA) impurity solver underestimates the Kondo temperature.

To solve the impurity problem in presence of an applied magnetic field we gave special attention to the off-diagonal terms in the impurity hybridization strength Δ , which give a significant contribution to the form factor.